

NONLINEAR ELASTIC-PLASTIC ANALYSIS AND POST-BUCKLING OF STEEL FRAMES WITH GUSSETED PLATE MEMBERS

Prof. Dr. Sabih Z. Al-Sarraf
Building and Construction Dept.
University of Technology

Asst. Prof. Dr. Jasim Al-Khafaji
College of Engineering
Almustansiriya University

Dr. Ali Sabah AL-Amili
College of Engineering
Almustansiriya University

Abstract

In this study, a theoretical analysis is presented for estimating the in-plane large displacement elastic-plastic stability behavior of steel frames having prismatic and non-prismatic members with end gusseted plates subjected to increasing static loads. The analysis adopts the beam-column approach and models the structural members as beam-column elements. The formulation of the beam-column element is based on Eulerian approach allowing for the influence of the axial force on bending stiffness.

In this study, the effect of gusseted plate is taken with the modified stability and bowing functions for gusseted plate with prismatic and non-prismatic members (Tapered and Non-linearly tapered). The post-buckling analysis is studied, and the incremental load control with different load increment strategies and the modified Newton-Raphson method with different iterative strategies are used to obtain the complete load-displacement curve. Furthermore, the determinant technique is used to detect the intersection of load limit points.

As a result, the beam column approach can be used in the analysis of plane frames with and without gussets and with any varying section. The ultimate load capacity can be increased with gusset-plate members, and with tapering the prismatic members for the same weight, and then the displacement can decrease.

Keywords: Nonlinear , Post-Buckling , Steel , Gusseted Plate

الخلاصة

(Critical Points)

Nomenclature

- A_O : Equivalent area of member.
 $C1, C2$: Stability functions of prismatic member.
 d : Depth of member.
 g : Gusseted length.
 I : Moment of inertia of member.
 L : Length of member.
 m : Shape factor.
 P : Applied load.
 Q : Axial load.
 U : Depth ratio

Introduction

Extensive research has been conducted on the non-linear analysis of steel structures in recent years. The recent development of limit state design methodologies, such as that of this study, is due to the widespread acceptance of the ultimate limit state design. The AISC "Load and Resistance Factor Design" (LRFD) specification [AL-Amili, 2005] has focused particular attention on more sophisticated analysis method than its older "Allowable Stress Design" specifications. In LRFD, steel frames need to be analyzed with respect to failure or ultimate Limit State. In the ultimate Limit State, the members are expected to have a large displacement and non-linear material behavior with axial and bending effects coupled together.

This study presents a derivation of the modified tangent stiffness matrix in the presence of plastic hinges for prismatic and non-prismatic members.

Modified Force-Displacement Relationships For Members With End Gusset Plates (Non-Prismatic Member)

The member of length (L) shown in **Figure (1)** is completely rigid over the length ends g1 and g2. The central length L_o has uniform or non-uniform flexural rigidity (E. I) is undeformed.

In this study, the non-prismatic member force-deformation relations, obtained from an application of the conventional beam- column theory by expressing the terminal bending moments (M1) and (M2) by rotations of θ_A and θ_B at A' and B' respectively[AL-Amili,2005]: -

$$M_1 = \frac{EI}{L_o} (\bar{\gamma}_1 \theta_A + \bar{\gamma}_2 \theta_B) \quad \dots (1)$$

$$M_2 = \frac{EI}{L_o} (\bar{\gamma}_2 \theta_A + \bar{\gamma}_3 \theta_B) \quad \dots (2)$$

$$Q = EA_o \left(\frac{\bar{u}}{L_o} - \bar{C}b \right) \quad \dots (3)$$

in which ($\bar{\gamma}_1$ and $\bar{\gamma}_2$) are stability functions for non-prismatic members (tapered or non-linearly tapered) with end gusset plates expressed in terms of (S1,Sc and S2) as shown in the following, and A_o : is equivalent area of non-prismatic member [AL-Damarchi,1999] and Cb: is the length correction factor due to bowing action which have been derived with the modified stability functions for member with gusset plates[1,2]:

$$\bar{\gamma}_1 = \frac{S_2}{U^m} + \frac{2g1}{L_o} \left(1 + \frac{g1}{L_o}\right) AG^* \quad \dots (4)$$

$$\bar{\gamma}_2 = \frac{Sc}{U^m} + \left(\frac{S1+Sc}{U^m}\right) \left(\frac{g1+g2}{L_o}\right) + \frac{2g1.g2}{L_o^2} .AG^* \quad \dots (5)$$

$$\bar{\gamma}_3 = \frac{S_1}{U^m} + \frac{2g1}{L_o} \left(1 + \frac{g1}{L_o}\right) AG^* \quad \dots (6)$$

where

$$AG^* = \frac{(S_1+Sc)}{U^m} - \frac{\pi^2}{2} q \quad \dots (7)$$

while U is the depth factor (U=d1/d2) and m is the shape factor for non-prismatic member (tapered or non-linearly tapered) [3,4,5].

where S_1, Sc and S_2 are modified stability function for non-prismatic member (tapered or non-linearly tapered) [3,4,5].

Where

$$q = \frac{Q}{QE} = \frac{Q.L_o^2}{\pi^2 .E .I1} \quad \dots (8)$$

Equation (8) can be rewritten as:

$$q = \frac{\bar{\lambda}^2}{\pi^2} \left(\frac{\bar{u}}{L_o} - \bar{C}b \right) \quad \dots \quad (9)$$

While
$$\bar{\lambda} = \frac{L_o}{\sqrt{I1/A_o}} = \frac{L_o}{r} \quad \dots \quad (10)$$

and $L_o = L - g1 - g2$

For non-prismatic member with gusset plates, assuming $\theta_A = \theta_{1,2}$ and $\theta_B = \theta_2$, then the derivation of the length correction factor due to bowing actions is shown below[1,2]: -

$$\bar{C}b = (\bar{\beta}_1.\theta_1^2 + 2\bar{\beta}_2.\theta_1.\theta_2 + \bar{\beta}_3.\theta_2^2)$$

where \bar{u} , $\bar{C}b$: are the modified axial deformation in a member with gusset plate due to axial force, and the length correction factor due to bowing action which have been derived with the modified stability functions, respectively, where g1 and g2 are gusset length[1,2]:

The derivation of modified bowing functions for a non-prismatic member which takes into account the effect of the gusset plates are shown below[1,2]:

$$\bar{\beta}_i = \frac{-\bar{\gamma}'_i}{2\pi^2} \quad i = 1,2,3 \quad \dots \quad (11)$$

while $\bar{\gamma}'_i$ is the first derivative of the stability function with gusset plates.

$$\bar{\gamma}'_1 = U^{(2-\phi).m/4} . \bar{C}'_1 \quad \dots \quad (12)$$

$$\bar{\gamma}'_2 = U^{(1-\phi).m/4} . \bar{C}'_2 \quad \dots \quad (13)$$

$$\bar{\gamma}'_3 = U^{-\phi.m/4} . \bar{C}'_1 \quad \dots \quad (14)$$

where ϕ is a factor depending on the shape factor and the degree of variation of the section (i.e. tapered or non-linearly tapered) [1,2,5]:

where:

\bar{C}'_i : is the first derivative of the modified stability function for prismatic member with gusset plates.

The modified bowing functions for a non-prismatic member with gusset plates become[1,2]

$$\bar{\beta}_1 = \frac{-U^{(2-\phi).m/4}}{2\pi^2} . \bar{C}'_1 \quad \dots \quad (15)$$

$$\bar{\beta}_2 = \frac{-U^{(1-\phi).m/4}}{2\pi^2} . \bar{C}'_2 \quad \dots \quad (16)$$

$$\bar{\beta}_3 = \frac{-U^{(-\phi).m/4}}{2\pi^2} . \bar{C}'_1 \quad \dots \quad (17)$$

while the modified stability functions for a prismatic member with gusset plates are[1,2]

$$\bar{C}_1 = C_1 + \frac{2g1}{L_o} \left(1 + \frac{g1}{L_o} \right) . Ag \quad \dots \quad (18)$$

$$\bar{C}_2 = C_2 + (C_1 + C_2) \left(\frac{g1 + g2}{L_o} \right) + \frac{2g1.g2}{L_o^2} . Ag \quad \dots \quad (19)$$

where C_1 and C_2 are stability functions for a prismatic member without gusset plates.

The tangent stiffness matrix for non-prismatic member (tapered and non-linearly tapered) with gusseted plate is derived as below[1,2] :

$$[t] = \frac{E.I_1}{L_o} \begin{vmatrix} \bar{\gamma}_1 + \frac{\bar{G}1}{\pi^2 \bar{H}} & \bar{\gamma}_2 + \frac{\bar{G}1.\bar{G}2}{\pi^2 \bar{H}} & \frac{\bar{G}1}{\bar{H}} \\ & \bar{\gamma}_3 + \frac{\bar{G}2^2}{\pi^2 \bar{H}} & \frac{\bar{G}2}{\bar{H}} \\ Symetric & & \frac{\pi^2}{\bar{H}} \end{vmatrix} \dots (20)$$

where :

$$\bar{G}1 = -2\pi^2 (\bar{\beta}_1.\theta_1 + \bar{\beta}_2.\theta_2) = \bar{\gamma}'_1.\theta_1 + \bar{\gamma}'_2.\theta_2 \dots (21)$$

$$\bar{G}2 = -2\pi^2 (\bar{\beta}_2.\theta_1 + \bar{\beta}_3.\theta_2) = \bar{\gamma}'_2.\theta_1 + \bar{\gamma}'_3.\theta_2 \dots (22)$$

$$\bar{H} = \frac{\pi^2}{\lambda^2} + (\bar{\beta}'_1.\theta_1^2 + 2\bar{\beta}'_2.\theta_1.\theta_2 + \bar{\beta}'_3.\theta_2^2) \dots (23)$$

$$L_o = L - g1 - g2 \dots (24)$$

Modified Tangent Stiffness Matrix for Simulation of Plastic Hinges[3]

In modifying the tangent stiffness matrix to include the inelastic effects on the member stiffness, the following assumptions are used:

- 1- The material is assumed to be ideally elastic-perfectly plastic.
- 2- Yielding is considered to be concentrated at member ends in the form of plastic hinges.
- 3- The members are assumed to remain elastic between plastic hinges.
- 4- Reversal of plastic hinge rotations is not taken into account.
- 5- The influence of axial force in the plastic moment capacity is taken into account.

The member stiffness relationships previously described are based on the assumption that each member is rigidly connected to joints at both ends. When plastic (or real) hinges are present, the relative member end rotations at the released ends are obtained from relative member force deformation relationships. Thus for a member with plastic hinge at end 1

$$\theta_1 = \frac{LM_{PC1}}{EI_1\gamma_1} - \frac{\gamma_2}{\gamma_1}\theta_2 \dots (25)$$

For a member with plastic hinge at end 2

$$\theta_2 = \frac{LM_{PC2}}{EI_1\gamma_3} - \frac{\gamma_2}{\gamma_3}\theta_1 \dots (26)$$

and for a member with plastic hinges at both ends

$$\theta_1 = \frac{L}{EI_1} \frac{(\gamma_3 M_{PC1} - \gamma_2 M_{PC2})}{(\gamma_1 \gamma_3 - \gamma_2^2)} \quad \dots (27)$$

$$\theta_2 = \frac{L}{EI_1} \frac{-(\gamma_2 M_{PC1} - \gamma_1 M_{PC2})}{(\gamma_1 \gamma_3 - \gamma_2^2)} \quad \dots (28)$$

In the case of real hinges at end i, $M_{pci}=0$ in Eqs. (25) to (28). For a prismatic member $M_{pci}=M_{pc2}=M_{pc1}$, $\gamma_1=\gamma_3=C_1$, and $\gamma_2=C_2$.

For a member with a plastic hinge at one end and a real hinge at the other, the relative member end rotations, θ_1 and θ_2 , can be expressed in terms of M_{pc1} or M_{pc2} and γ_1, γ_2 and γ_3 by using Eqs (27) and (28). For example, for a member with a real hinge at end 1 and a plastic hinge at end 2

$$\theta_1 = \frac{L}{EI_1} \frac{-\gamma_2 M_{PC2}}{(\gamma_1 \gamma_3 - \gamma_2^2)} \quad \dots (29)$$

$$\theta_2 = \frac{L}{EI_1} \frac{\gamma_1 M_{PC2}}{(\gamma_1 \gamma_3 - \gamma_2^2)} \quad \dots (30)$$

The tangent stiffness matrix in local coordinates, [t], can be developed for a member with hinges by eliminating the released coordinate and differentiating the resulting relation term by term, with respect to the remaining coordinates.

If incremental changes in the plastic moment capacities are neglected, i.e. plastic hinges are treated as real hinges, the non-zero elements of the 3x3 matrix, [t], thus obtained are:

For a member with a hinge at end 1

$$t_{22} = Z_{22} - Z_{12}^2/Z_{11} \quad \dots (31a)$$

$$t_{23} = t_{32} = Z_{23} - Z_{12}Z_{13}/Z_{11} \quad \dots (31b)$$

$$t_{33} = Z_{33} - Z_{12}^2/Z_{11} \quad \dots (31c)$$

For member with a hinge at end 2

$$t_{11} = Z_{11} - Z_{12}^2/Z_{22} \quad \dots (32a)$$

$$t_{13} = t_{31} = Z_{13} - Z_{12}Z_{23}/Z_{22} \quad \dots (32b)$$

$$t_{33} = Z_{33} - Z_{23}^2 / Z_{22} \quad \dots (32c)$$

And for a member with hinges at both ends

$$t_{33} = EA_0L \quad \dots (33)$$

In Eqs. (31) and (32), $[Z]$ is the local tangent stiffness matrix, the local tangent stiffness matrices as given by Eqs (31) to (33) can be used for members with real as well as plastic hinges. As indicated previously, incremental changes in the plastic moment capacities are not included in Eqs. (31) to (33) (i.e. $\Delta M_{pci}=0$)

In addition, Eq (33) (for a member with releases at both ends) assumes that the effect of incremental changes in the flexural bowing term on member axial force is negligible (i.e. $\Delta C_b=0$). It should be noted that these simplifications are limited to the tangent stiffness matrices and do not extend to the system equilibrium equations.

As the order of $[t]$ is (3x3) even in the presence of member releases, the transformations can be used to obtain the tangent stiffness matrix, $[T]$, in the global system[1,3,5].

Effect of Axial Force on Plastic Moment Capacity:

When a steel frame undergoes a large plastic deformation, plastic hinges are expected to form. The plasticity can be concentrated or distributed. In the distributed model, plastification may occur across the cross-section and along the length of the member.

Consideration of distributed plasticity is computationally expensive[1,3,5]. Concentrated rather than distributed plasticity is used in the formulation so as to reduce the complexity of the problem and to minimize the cost and time required for the solution procedure. The reduction of the plastic moment capacity is presented. In a non-prismatic member the plastic moment capacity varies along the length. The plastic section modulus of a non-prismatic member with linear variation of cross section can be presented as follows: -

$$(Z_P)_X = Z_{P2} \left[1 + (U-1) \left(\frac{\bar{X}}{L} \right) \right]^{mZ} \quad \dots (34a)$$

The plastic section modulus of a non-prismatic member with non-linear variation of parabolic type is:

$$(Z_P)_X = Z_{P2} \left[1 + (U-1) \left(\frac{\bar{X}}{L} \right)^2 \right]^{mZ} \quad \dots (34b)$$

For cubic type:

$$(Z_P)_X = Z_{P2} \left[1 + (U-1) \left(\frac{\bar{X}}{L} \right)^3 \right]^{mZ} \quad \dots (34c)$$

in which “mz” is a shape factor that depends on the cross-sectional shape, tapering ratio (U), and dimensions of the member

$$mZ = \log \left[\frac{Z_{P1}}{Z_{P2}} \right] / \log U \quad \dots (35)$$

where:

Z_{P1} = plastic section modulus at end 1

Z_{P2} = plastic section modulus at end 2

U = tapering ratio.

The reduced plastic moment capacity along the length of a non-prismatic member may be written as:

$$(M_{PC})_X = M_{PC2} \left[1 + (U-1) \left(\frac{\bar{X}}{L} \right)^k \right]^{mc} \quad \dots (36)$$

where:

k = 1 for linear variation, k = 2 for parabolic, and k = 3 for cubic. In which “mc” is a shape factor that depends on the cross-sectional shape, tapering ratio, and dimensions of the member.

$$mc = \log \left[\frac{M_{PC1}}{M_{PC2}} \right] / \log(U) \quad \dots (37)$$

where:

M_{PC1} = reduced plastic moment capacity at end 1

M_{PC2} = reduced plastic moment capacity at end 2

U = tapering ratio

Calculation of Member Axial Force⁽¹⁾:

The expression of the member axial force Q, involves bowing functions β_1 , β_2 , and β_3 , which in their turn, are functions of the axial force parameter q_1 .

In the presence of hinges, the problem is further complicated by the fact that the rotations at the released ends (Eqs (25) to (30)) are also functions of Q.

Then the correction factor for bowing, C'_b is given by

$$C'_b = \beta'_1 \theta_1 + 2\beta'_2 \theta_1 \theta_2 + \beta'_3 \theta_2^2 + 2\beta_1 \theta_1 \theta'_1 + 2\beta_3 \theta_2 \theta'_2 + 2\beta_2 (\theta_1 \theta'_2 + \theta'_1 \theta_2) \dots (38)$$

in which θ'_1 terms = zero at member ends rigidly connected to the joints. The rotations at such rigid ends are defined by the global joint displacements and remain constant during this iteration process.

For a member with hinges, θ'_1 terms at the released ends are given by differential of Eqs (25) to (28) with respect to q_1 . Thus, for a member with a plastic hinge at end 1

$$\theta'_1 = \frac{L}{EI_1 \gamma_1^2} (M'_{PC1} \gamma_1 - M_{PC1} \gamma'_1) - \frac{\theta_2}{\gamma_1^2} (\gamma_1 \gamma'_2 - \gamma_2 \gamma'_1) \dots (39)$$

For a member with a plastic hinge at end 2

$$\theta'_2 = \frac{L}{EI_1 \gamma_3^2} (M'_{PC2} \gamma_3 - M_{PC2} \gamma'_3) - \frac{\theta_1}{\gamma_3^2} (\gamma_3 \gamma'_2 - \gamma_2 \gamma'_3) \dots (40)$$

And for a member with plastic hinges at both ends

$$\theta'_1 = \frac{L}{EI_1 (\gamma_1 \gamma_3 - \gamma_1^2)^2} \left[(\gamma_1 \gamma_3 - \gamma_1^2) (M'_{PC1} \gamma_3 + M_{PC1} \gamma'_3 - M'_{PC2} \gamma_2 - M_{PC2} \gamma'_2) - (M_{PC1} \gamma_3 - M_{PC2} \gamma_2) (\gamma_1 \gamma'_3 + \gamma_3 \gamma'_1 - 2\gamma_2 \gamma'_2) \right] \dots (41)$$

And

$$\theta'_2 = \frac{L}{EI_1 (\gamma_1 \gamma_3 - \gamma_1^2)^2} \left[(\gamma_1 \gamma_3 - \gamma_2^2) (M'_{PC2} \gamma_1 + M_{PC2} \gamma'_1 - M'_{PC1} \gamma_2 - M_{PC1} \gamma'_2) - (M_{PC2} \gamma_1 - M_{PC1} \gamma_2) (\gamma_1 \gamma'_3 + \gamma_3 \gamma'_1 - 2\gamma_2 \gamma'_2) \right] \dots (42)$$

In these equations the values of M'_{Pci} can be determined by differentiation of the reduced moment capacity with respect to q_i .

Post-buckling Analysis

It is the consequence of any discrete formulation (e.g. the finite element method), that the deformation of a given structure is described by a set of (N) deformation parameters, which are also called generalized coordinates. In this context, the load – deformation history of a structure presents itself as a curve in a (N + 1) dimensional space spanned by the deformation parameters and the magnitude of the applied loads. Such a curve is usually referred to as equilibrium path or deformation path. The problem of elastic stability is intimately connected with singularities that occur somewhere along the path under consideration. These singular points are better known as critical points. Well known is their classification into limit points and bifurcation points. In principle, the elastic stability formulations should be relevant to the problem at hand and should have the capability of:

Computing the critical points, i.e. limit or bifurcation points
Tracing parts of the path or paths (branches) connected with these points.

From another point of view, the method should have the capability of computing post-buckling. It is clear now that there are two distinct strategies required for the successful completion of a single load increment in an incremental– iterative method:
Selection of a suitable external load increment for the first iterative cycle. The chosen increment is termed as an initial load increment and a particular strategy used to determine it is termed a load incrementation strategy.

Selection of an appropriate iterative strategy for application in subsequent iterative cycles with the aim of restoring equilibrium as rapidly as possible. If iterations are performed on the load parameter as well as the nodal displacement, an additional constraint equation involving the change in the load parameter is required. It is the form of this constraint equation that distinguishes the various iterative strategies.

Convergence Criteria:

A dimensionless convergence criterion is used which decides whether a sufficient accuracy has been achieved (thus when no further iterations are necessary). Commonly there are three types of convergence criteria. These are given as follows:

1. Unbalanced Force Vector Criterion:

This criterion depends on comparison between the internal force vector and external force vector, in other words, searching for a vector called unbalanced force vector to be small within a prescribed tolerance. In applying this criterion the resultant force and moment vector of the joints are treated separately and the convergence is assumed to have occurred when the inequality.

$$\left| \frac{\{P\}_i - \{F\}_i}{\{P\}_i} \right| \leq \text{tol} \quad \dots (43)$$

is satisfied, in which $\{P\}_i$ = resultant external force vector

$\{F\}_i$ = resultant internal force vector

$\{P\}_i - \{F\}_i$ = resultant unbalance force vector to be satisfied simultaneously and independently for each group .

2. Work Done Criterion:

This method uses a comparison between the work done by the internal forces and the external forces and convergence occurs when the inequality:

$$\left| \frac{W_e - W_i}{W_i} \right| \leq \text{tol.} \quad \dots (44)$$

is satisfied.

3. Displacement Criterion:

This criterion depends on comparison of the incremental values of $\{\Delta X\}$ of the displacements to their accumulative values $\{X\}$. In applying this criterion, translations and rotations of the joints are treated either as separated or mixed groups and convergence is assumed to have occurred when the following inequality is satisfied:

$$\left[\frac{\sum_i (\Delta X_i)^2}{\sum_i (X_i)^2} \right]^{1/2} \leq \text{tol.} \quad \dots (45)$$

In Eqs. (43) to (45) the dimensionless quantity, (tol.) represents a prescribed tolerance.

In this study the tolerance used as an indication for satisfied equilibrium condition is 0.001 for force and work criterion.

Results and Discussions:

1. Without Gusseted Member:

EX.1: One- bay Two – story Frame:

The geometrical and material properties as well as loading conditions are shown in **Figure (2)**.

Wong and Tin-Loi [1990] presented a novel method suitable for the incremental path dependent computer analysis of elastic – perfectly plastic frames including the effects of large deformation and analyzed this structure with effect of both geometrical and material non-linearity. In this study, the large displacement elastic-plastic stability and post-buckling analysis are made to this frame. **Figure (3)** shows the load-displacement curves for these analyses, and very good agreement is seen between the results of this study and those of the other previous reference [Wong and Tin-Loi,1990] . **Figure (4)** illustrates the degradation of the system tangent stiffness matrix as the load increases. This degradation becomes considerably large after the formation of the first plastic hinge, which gives an indication about the increase in the frame instability. The sequence of plastic hinge formation is shown in **Figure (5)**.

EX.2: Pitched Roof Frame:

Figure (6) shows the geometry, material properties and loading conditions for this example. [Kassimali,1983] analyzed the same problem. The results of the two analyses are shown in **Figure (7)**. An excellent agreement is seen between the two analyses.

The sequence of plastic hinge formation is shown in **Figure (8)**. It is noticed in this case that failure occurs after the formation of the five plastic hinges, i.e., failure occurs due to mechanism collapse.

From the load-determinant curve for this frame, which is shown in **Figure (9)**, it is noticed that the stiffness of the structure is reduced considerably after plastic hinge formation, and the decrease in stiffness continues up to failure.

2. With Gusseted Member

EX.3: Prismatic Beam with Gusset:

Figure (10) shows the geometry and load of this example. Many cases are taken to represent the supports, case (a) for fixed-fixed ends supports, case (b) for hinged-hinged ends supports and case (c) for fixed-hinged support. All these cases are taken with different values of gusset lengths. The modified stability and bowing functions which are derived in this study are used in this example by 1-element for half the beam because it is symmetrical. The results of load-displacement curves for these cases and gusset lengths are shown in Figure (11), (case (a), case (b) and case (c)). The plastic hinge positions are done in the distance of gusset length from point A and C, and in point B for case (a). For case (b), it is done in point B. For case (c), they are done in the distance of gusset length from point C., and in point B.

EX.4 : Non-Prismatic Parabolic Section Beam With Gusset:

Figure (12) shows the geometry and loading of this example. This example is analyzed for three cases of supports and different gusset lengths. The non-prismatic section of tapered ratio ($U=2$) and parabolic distribution are shown in Fig. (12). The modified stability and bowing function [AL-Amili,2005][Faris,2002]^(1,5) are used and one element for half the beam because it is symmetrical. The load-displacement curves for different support conditions and gusset lengths are shown in Fig. (13), (case (a), case (b) and case(c)). The plastic hinge positions are done in the distance of gusset length from point A and C, and in point B for case (a). For case (b), it is done in point B. For case (c) they are done in the distance of gusset length from point A., and in point B.

Conclusion:

1. The gusseted plate increases the load capacity of the frame and this is dependent on the gusset length and the varying sections of the member. These ratios are about (8-40) %.
2. The plastic hinge position for a gusseted member is produced at the distance of gusset length from the fixed support.
3. The gusseted plate taken the same behavior of support, which contact with it, therefore, the plastic hinge not appears when the support is pin.
4. increasing the gusseted ratio causes increase in the capacity of member and this behavior is low appearance when the supports are pin
5. using one element with gusseted plate gives good agreements in his study and produces higher advantage of the soft ware.

References

- 1- AL-Amili, "Large Displacement Elastic and Elastic-Plastic Analysis And Post-buckling of Steel Frames with Varying Non-prismatic Members and Gusseted Plates", Ph.D. Thesis, University of AL- Mustansiriya, Iraq, 2005.
- 2- AL-Sarraf, Al-Khafaji and AL-Amili "Nonlinear Elastic Analysis And Postbuckling of Steel Frames with Non-prismatic Gusseted Plate Members".
- 3- AL-Damarchi, H.T., "Large Displacement Elastic-Plastic Analysis of Non Prismatic Members", *Ph.D. Thesis, University of Technology, Iraq, 1999.*
- 4- AL-Sarraf, "Elastic Instability of Frames with Uniformly Tapered Members", *The Structural Engineering, March 1979, pp. 18-24.*
- 5- Faris, "Large Displacement Elastic-Plastic Analysis of Plane Frames with Non-Prismatic Members of Non-linearly Varying Sections", Ph.D. Thesis, University of Technology, Iraq, 2002.
- 6- Wong, M.B. and Tin-Loi, F., "Analysis of Frames Involving Geometrical And Material Non-Linearities", *International Journal of Computers and Structural*, Vol. 34, No. 4, 1990, pp. 641-646.
- 7- Kassimali, A., "Large Deformation Analysis of Elastic-Plastic Frames", *Journal of Struc. Engineering*, ASCE, Vol. 109, No.ST 8, Aug., 1983, pp. 1869-1886.

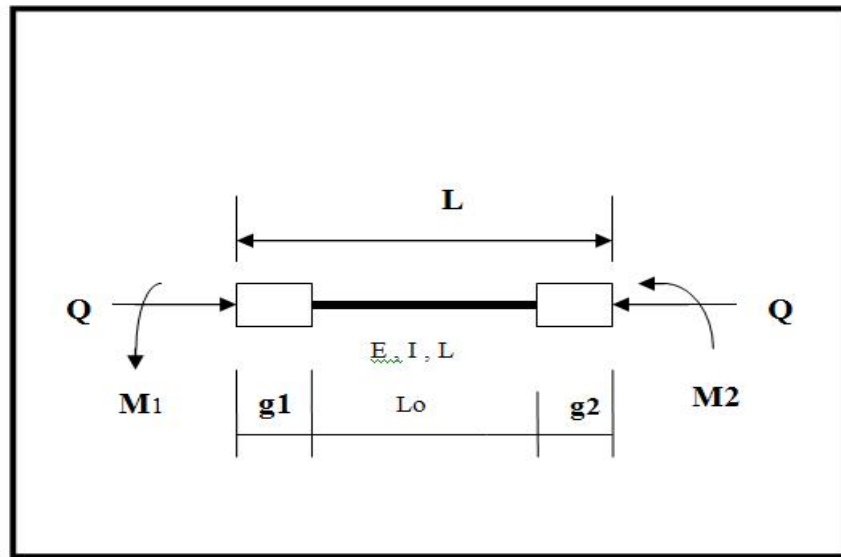


Fig. (1): Relative forces in local coordinates for a member with gusset plates.

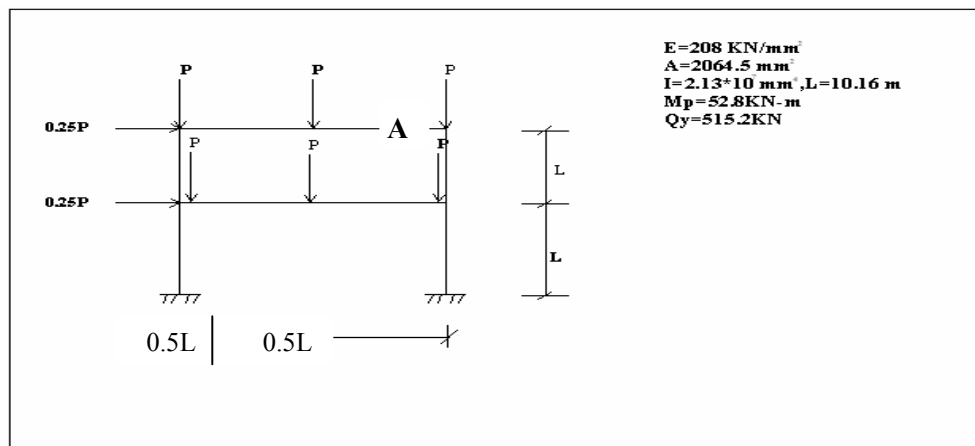


Fig. (2): Geometry and loading.

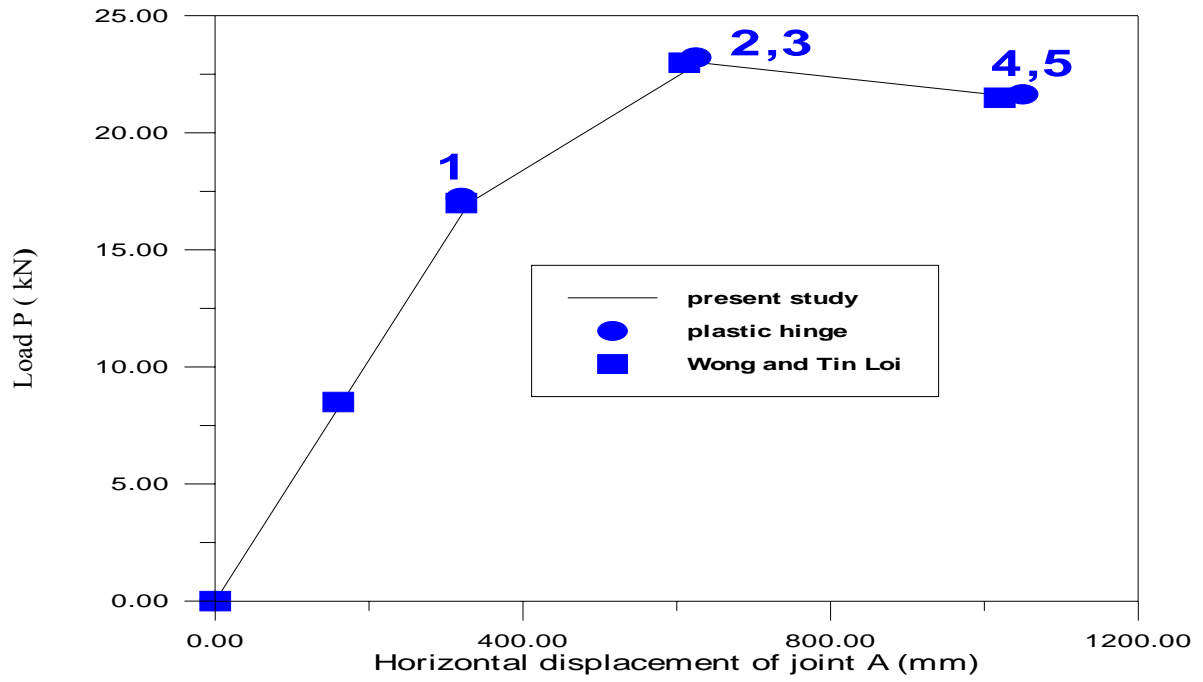


Fig. (3): Load-displacement curves.

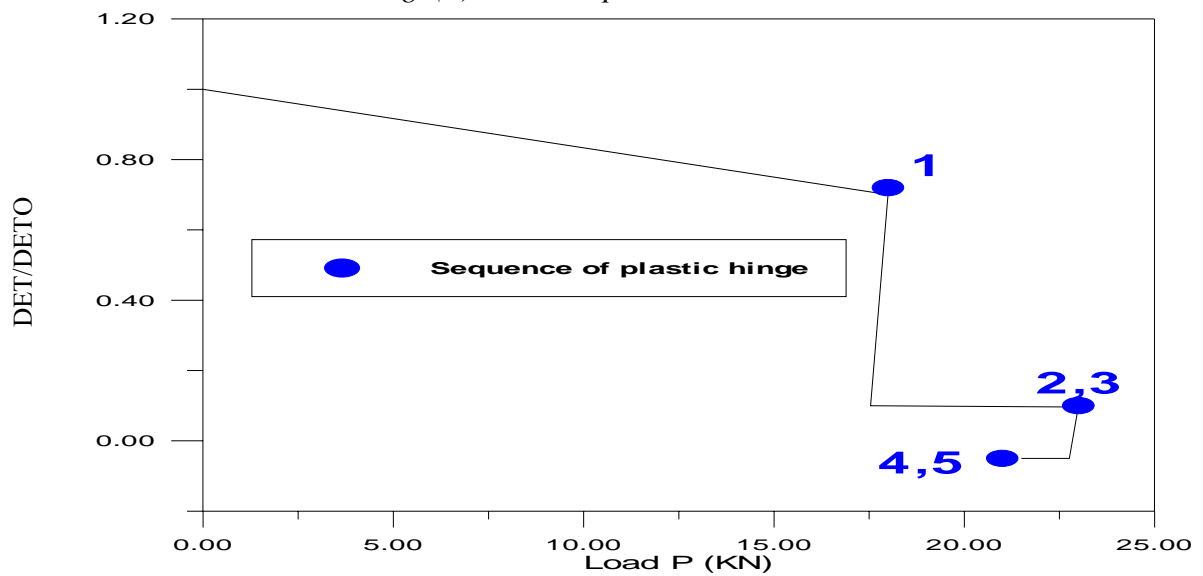


Fig. (4): Load-determinant ratio curve.

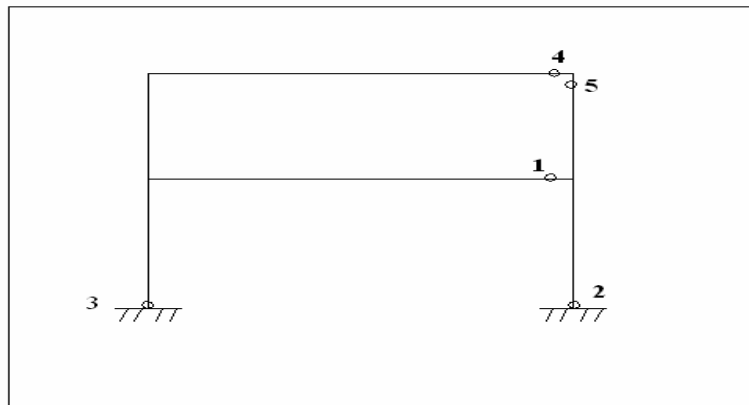


Fig. (5): Sequence of plastic hinge formation.

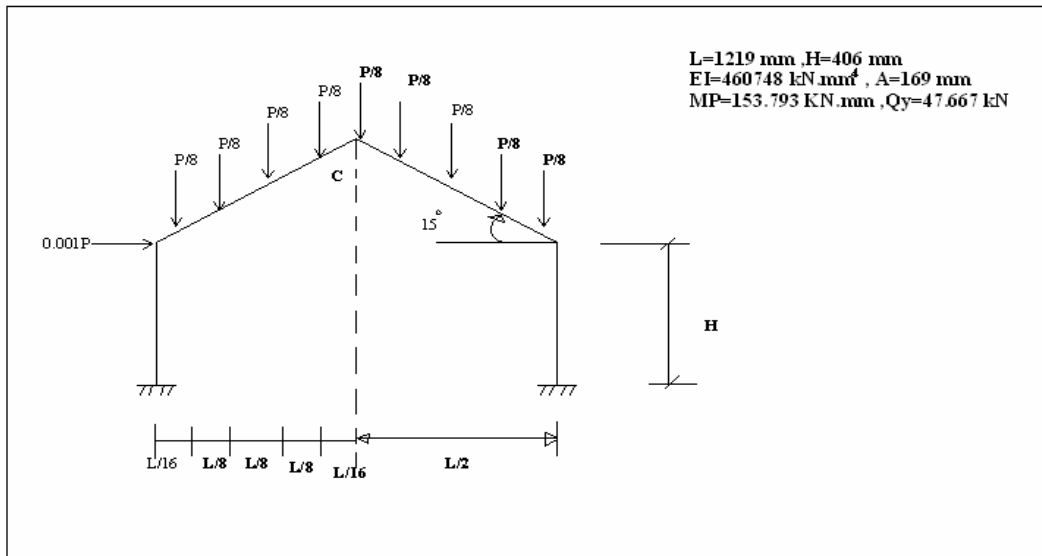


Fig. (6): Geometry and loading.

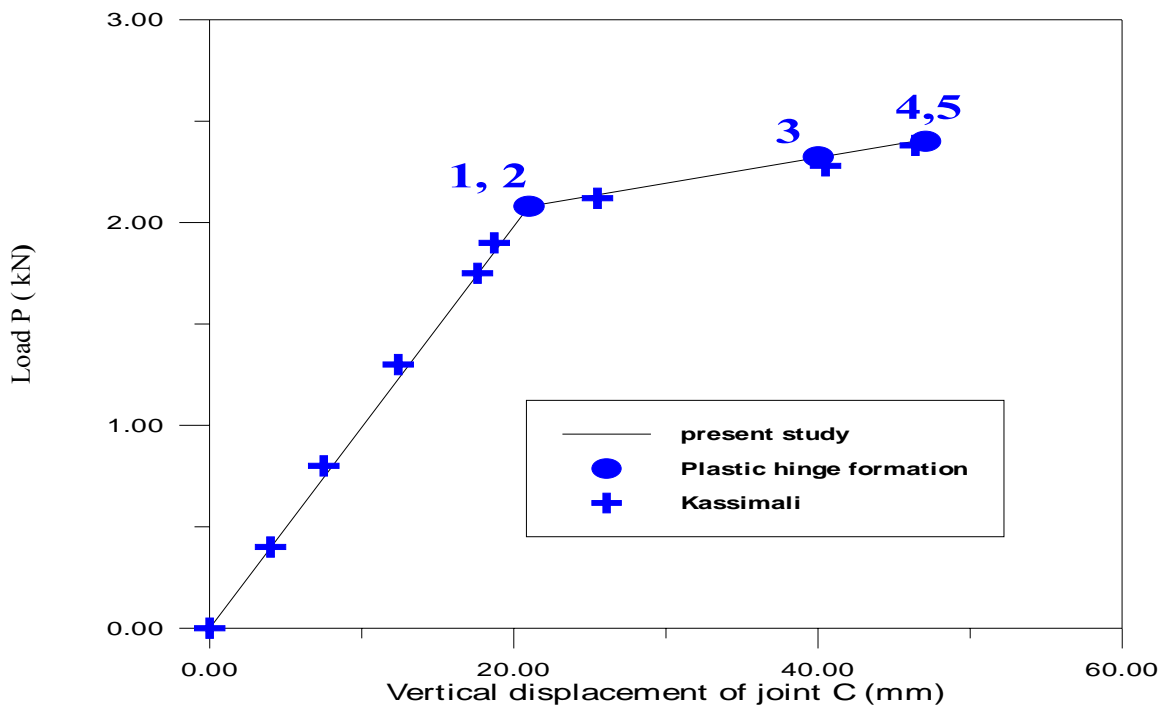


Fig. (7): Load-displacement curves.

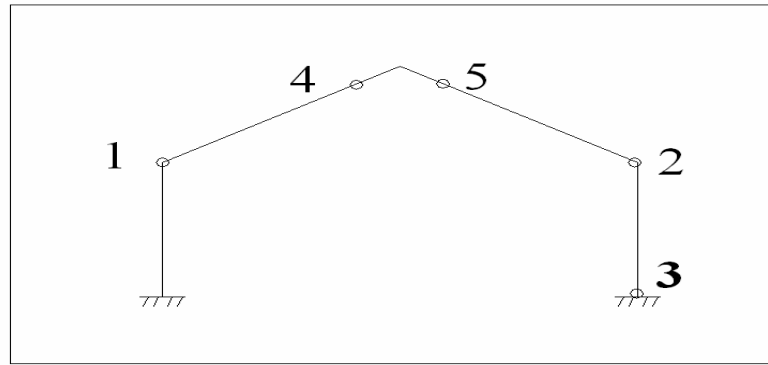


Fig. (8): sequence of plastic hinge formation.

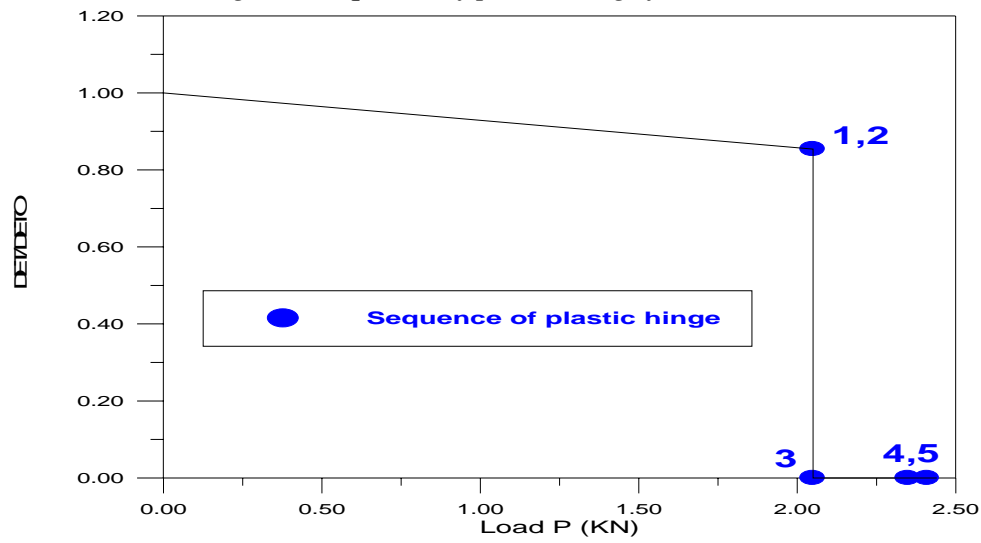


Fig. (9): Load-determinant ratio curve.

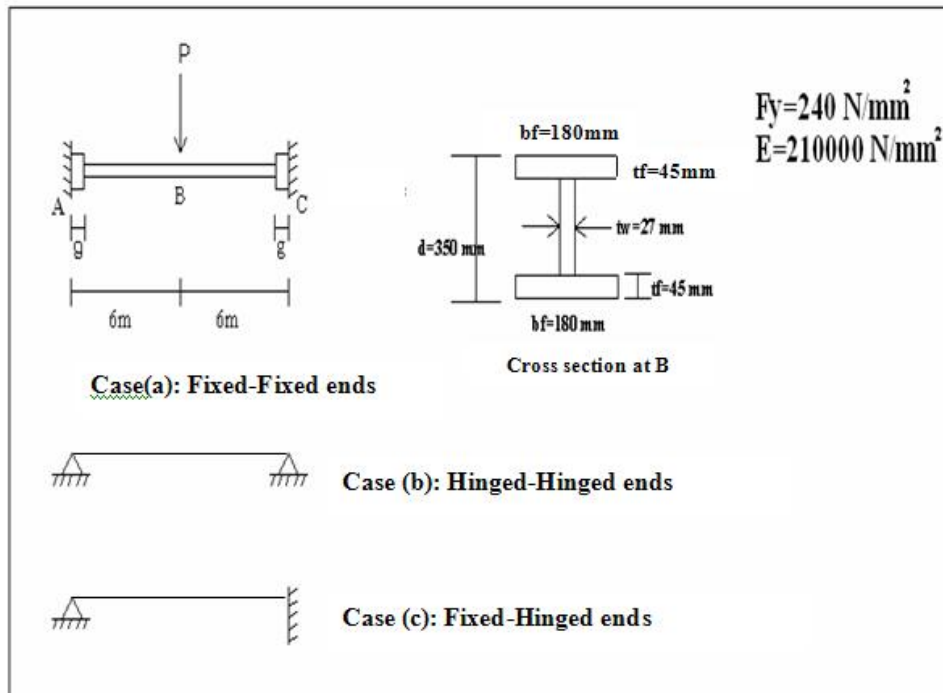


Fig. (10): Geometry and loading.

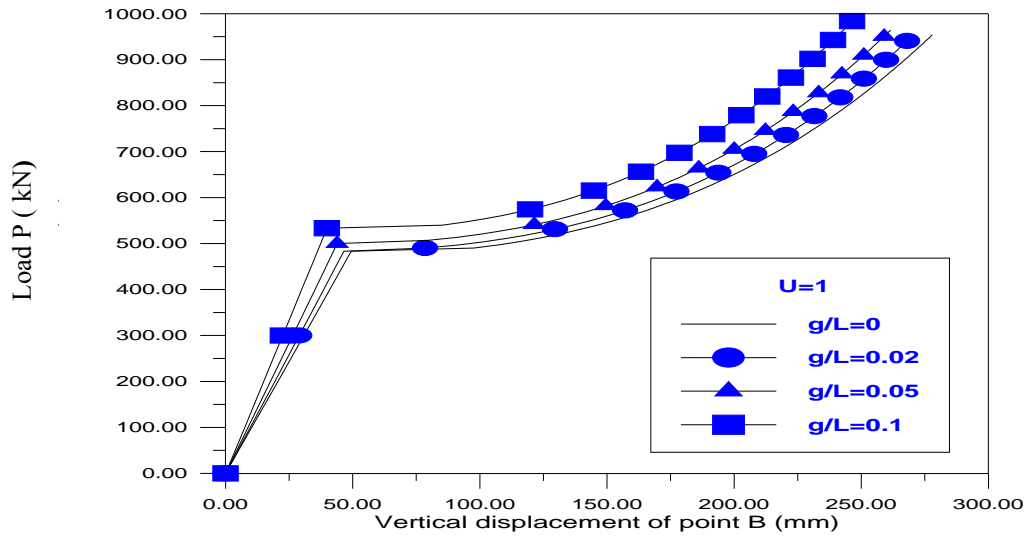
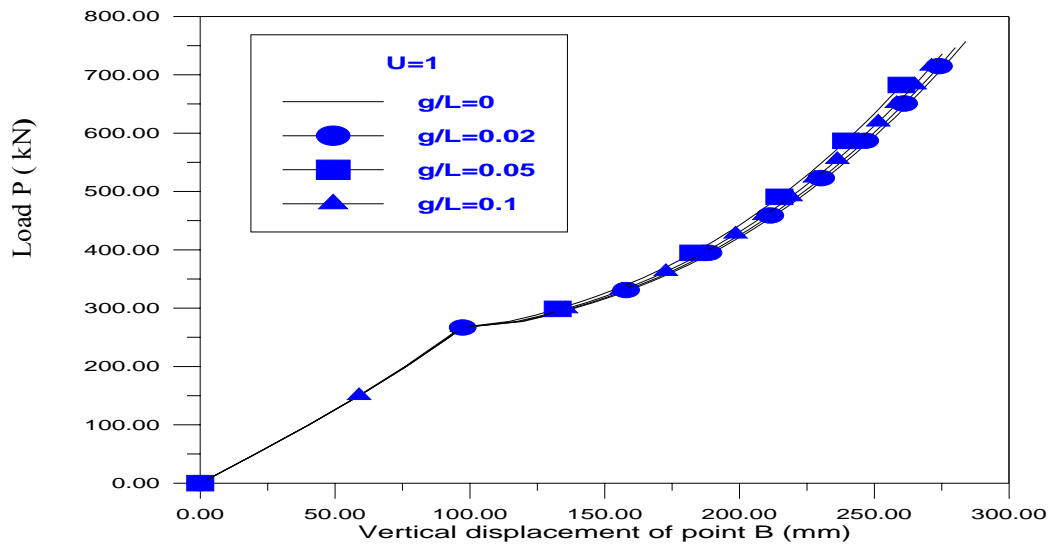
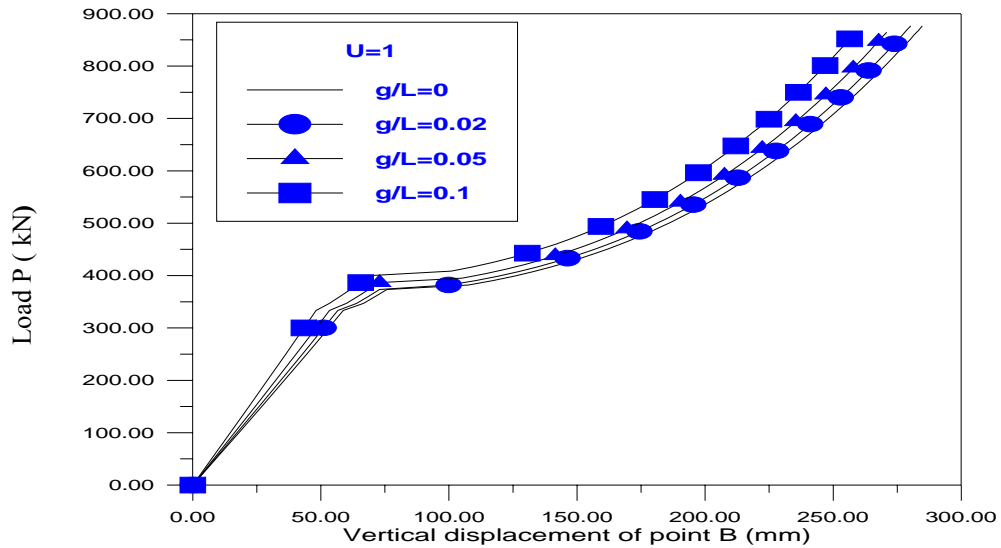


Fig. (11): Case (a) Fixed-Fixed ends.



Case (b) Hinged-Hinged ends.

Fig. (11): Load- displacement curves, Case (a,b and c).



Case (c) Fixed-Hinged ends.

Fig. (11): Continued.

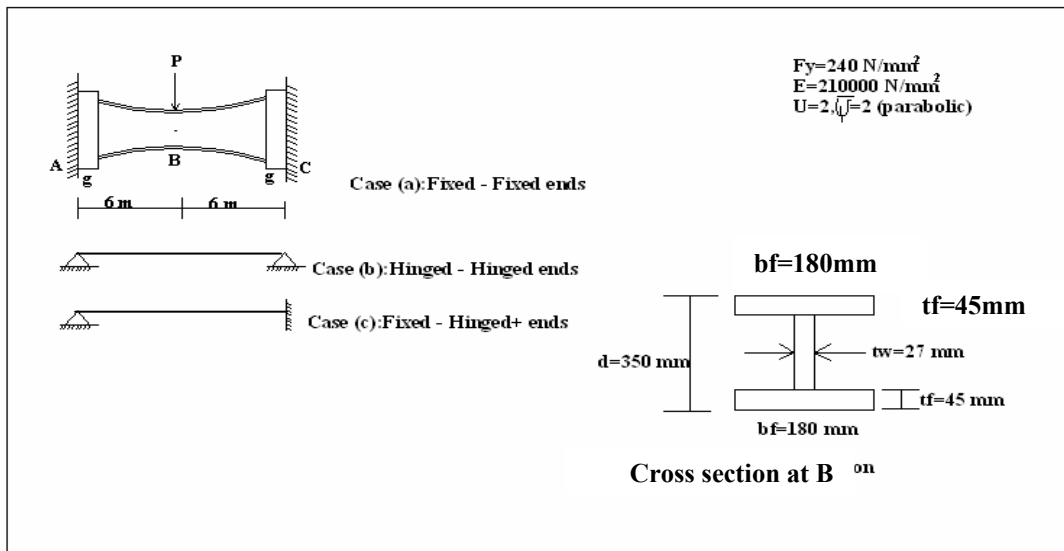
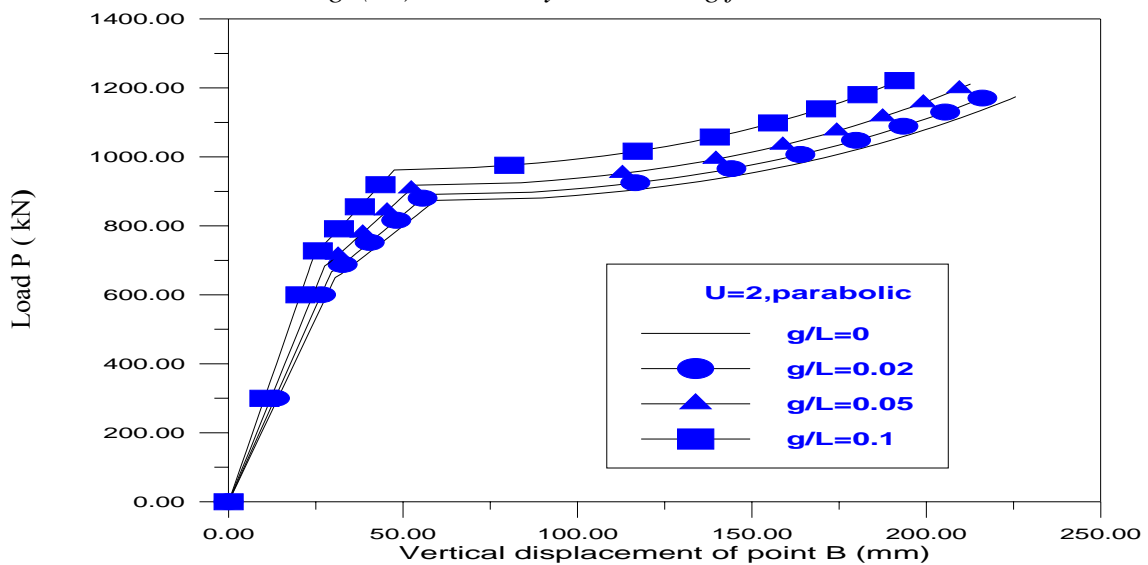
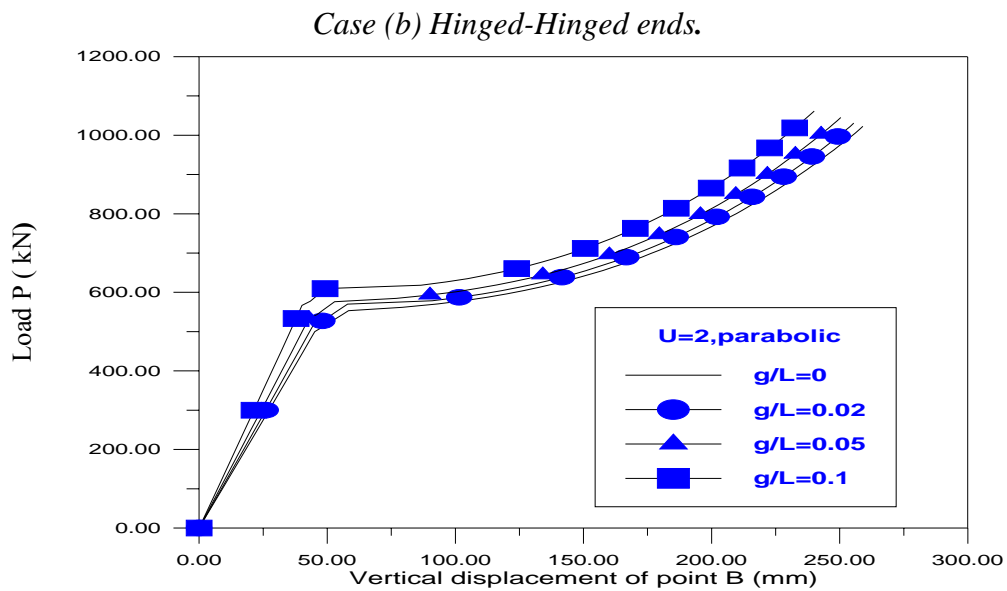
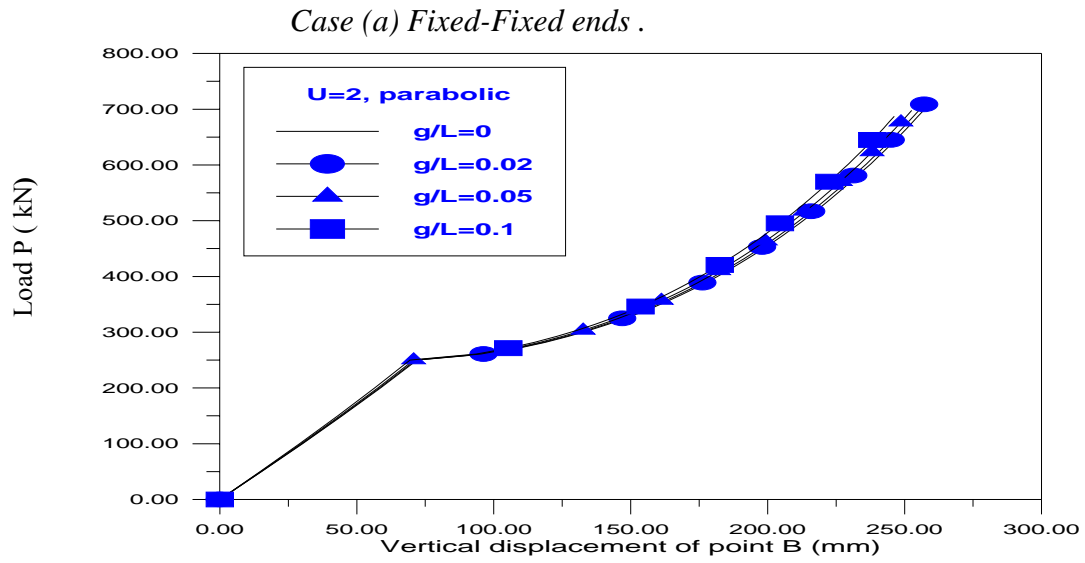


Fig. (12): Geometry and loading for Ex. 4.





Case (c) Fixed-Hinged ends.

Fig. (13): Load- displacement curves, (case (a, b and c)).